Impacts of Climate Change on the Growing Season in the United States

Daniel E. Christiansen*

U.S. Geological Survey, Iowa Water Science Center, Iowa City, Iowa

Steven L. Markstrom and Lauren E. Hay

U.S. Geological Survey National Research Program, Lakewood, Colorado

Received 13 August 2010; accepted 26 March 2011

ABSTRACT: Understanding the effects of climate change on the vegetative growing season is key to quantifying future hydrologic water budget conditions. The U.S. Geological Survey modeled changes in future growing season length at 14 basins across 11 states. Simulations for each basin were generated using five general circulation models with three emission scenarios as inputs to the Precipitation-Runoff Modeling System (PRMS). PRMS is a deterministic, distributed-parameter, watershed model developed to simulate the effects of various combinations of precipitation, climate, and land use on watershed response. PRMS was modified to include a growing season calculation in this study. The growing season was examined for trends in the total length (annual), as well as changes in the timing of onset (spring) and the end (fall) of the growing season. The results showed an increase in the annual growing season length in all 14 basins, averaging 27–47 days for the three emission scenarios. The change in the spring and fall growing season onset and end varied across the 14 basins, with larger increases in the total length of the growing season occurring in the mountainous regions and smaller increases occurring in the Midwest, Northeast, and Southeast regions. The Clear Creek basin, 1 of the 14 basins in this study, was

* Corresponding author address: Daniel E. Christiansen, U.S. Geological Survey, Iowa Water Science Center, 400 S. Clinton St., Iowa City, IA 52240.

E-mail address: dechrist@usgs.gov

DOI: 10.1175/2011EI376.1

evaluated to examine the growing season length determined by emission scenario, as compared to a growing season length fixed baseline condition. The Clear Creek basin showed substantial variation in hydrologic responses, including streamflow, as a result of growing season length determined by emission scenario.

KEYWORDS: Growing season; Climate change; PRMS model

1. Introduction

Climate simulations by the Intergovernmental Panel on Climate Change (IPCC) have demonstrated warming of the surface of Earth from 1860 to 2000 (Houghton et al. 2001). The simulated climatic changes show a significant impact on growing season length (GSL) leading to corresponding changes to important hydrologic cycles in the watershed-scale hydrologic cycle.

GSL, the onset of spring warming, the delay in fall cooling, and basin hydrology are integrally linked. GSL has been shown to affect hydrologic factors such as snowmelt and runoff (Backlund et al. 2008). In areas of the western United States, a shift in the onset of snow and the timing of snowmelt can affect water availability related to drinking water, hydroelectric power, and fish reproduction (Barnett et al. 2005). In addition, a change in the GSL can alter the hydrologic cycle by increasing evapotranspiration, depleting soil moisture, and reducing streamflow (Backlund et al. 2008). Along with hydrologic effects, the GSL is traditionally associated with crop production and impacts on crop yields. For any agricultural commodity, variation in yield between years is related to the growing season weather (Backlund et al. 2008). Such a change in GSL could translate to a corresponding change in water usage, that is, an increase in usage due to a longer growing season or a decrease due to a shorter period for crops to reach maturity (Backlund et al. 2008).

As with agriculture, GSL affects forested areas. Forest growth appears to be increasing in regions of the United States where tree growth is normally limited by low temperatures and short growing seasons (McKenzie et al. 2001; Joos et al. 2002; Caspersen et al. 2000). In the semiarid forests of the southwest, however, forest growth has been decreasing because of drought effects and longer warm periods (McKenzie et al. 2001; Joos et al. 2002; Caspersen et al. 2000). Some forest types within the United States such as oak/hickory are projected to expand, and others such as maple/beech/birch are predicted to contract. The spruce/fir is likely to disappear altogether with increasing temperatures (Ryan et al. 2008; Fagre et al. 2009).

A change in the GSL can also dramatically influence biologic territories and life cycles (Logan et al. 2003). Increasing GSL has been related to changes in migratory bird patterns, increased insect infestation, and changes in habitat (Janetos et al. 2008). A study of bird migration has documented that birds wintering in the southern United States now arrive back in the Northeast an average of 13 days earlier than they did between 1900 and 1950, and birds wintering in South America arrive back in the Northeast an average of 4 days earlier (Janetos et al. 2008). Phenological studies have shown that the increase in GSL caused by warmer air temperatures have caused many species of animals and plants to expand their geographic ranges poleward in latitude and upward in elevation over the past century (Haggerty and Mazer 2008). In an analysis of 866 peer-reviewed papers

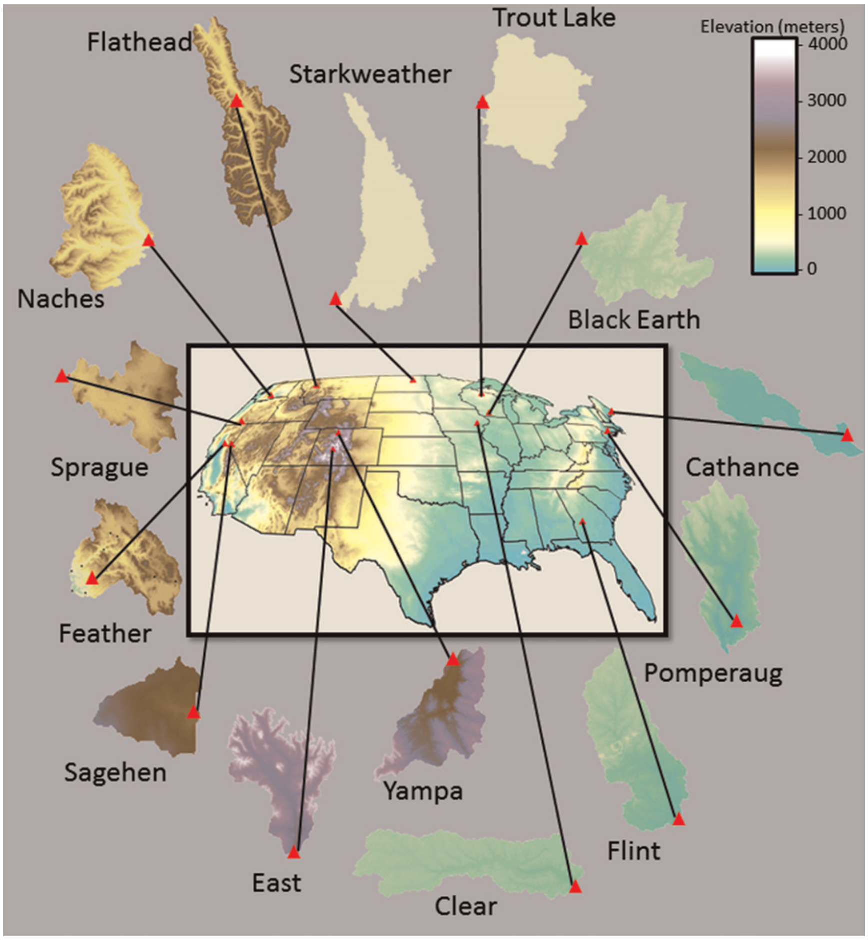

Figure 1. Location map of the United States showing the 14 selected basins. Red triangle denotes location of stream gauge for model calibration (basins not to scale; see Table 1 for relative scales).

exploring the ecological consequences of climate change, nearly 60% of the 1598 species studied exhibited shifts in their distributions and/or phenologies over the 20- and 140-yr time frames (Parmesan and Yohe 2003). For example, the pine beetle has expanded its range into regions previously too cold to support its survival because of increases in temperatures and growing seasons (Carroll et al. 2003). These biological shifts in spatial and temporal range are being called the ‘‘fingerprint of climate change’’ (Haggerty and Mazer 2008). There are many aspects of the ecosystem the GSL can affect across the United States and the world.

This paper focuses on the potential impacts that climate change can have on GSL and the hydrologic cycles of 14 selected basins across the United States. The basins are shown in Figure 1 and listed by drainage area in Table 1. General circulation models (GCMs) are used to determine emission scenarios as input into the Precipitation-Runoff Modeling System (PRMS).

Table 1. Selected basins listed by drainage area.

Region	Basin name	Basin abbreviation	USGS Gauge No.	Gauge drainage area (km^2)	Reference to previous work
Cascade	Naches River below Tieton River, WA	Naches	12494000	2437	Mastin and Vaccaro 2002
	Sprague River near Chiloquin, OR	Sprague	11501000	4053	Hay et al. 2006b; Hay et al. 2009
Sierra Nevada	Sagehen Creek near Truckee, CA	Sagehen	10343500	27	Markstrom et al. 2008
	Feather River, CA	Feather	—	9324	Koczot et al. 2005
	Middle Fork of the Feather River near Merrimac, CA*		11394500	2751	Koczot et al. 2005
Rockies	South Fork of the Flathead River, MT	Flathead	12362500	4307	—
	East River at Almont, CO	East	9112500	748	McCabe and Hay 1995
	Yampa River at Steamboat Springs, CO	Yampa	9239500	1471	Hay et al. 2006a; Hay et al. 2006c
Midwest	Starkweather Coulee near Webster, ND	Starkweather	5056239	543	Vining 2002
	Black Earth Creek at Black Earth, WI	Black Earth	5406500	118	—
	Clear Creek near Coralville, IA	Clear	5454300	254	—
	Trout River at Trout Lake, WI	Trout Lake	5357245	120	—
Northeast	Cathance Stream at Edmunds, ME	Cathance	1021230	85	Dudley 2008
	Pomperaug River at Southbury, CT	Pomperaug	1204000	194	Bjerklie et al. 2010
Southeast	Flint River at Montezuma, GA	Flint	2349500	7511	Viger et al. 2010

* Middle Fork is a gaged interior basin of the Feather River basin.

2. Growing season length definition

Numerous studies quantifying GSL have been completed in the United States. The studies examine GSL using a variety of methods such as statistical methods, phenological events, and climatological indicators. The U.S. Department of Agriculture's National Agricultural Statistics Service defines the GSL as the time between the last and first freezing air temperatures. The first and last freezing temperatures have been used in many studies (Wang 1963; Brinkman 1979; Cooter and LeDuc 1995; Kunkel et al. 2004). The GSL can also be defined as the period between the last hard frost in the spring and the first hard frost in the fall. Hard frost is defined as daily minimum temperature necessary to kill 50% of exposed plants (Baron et al. 1984). GSL has also been defined as the period between the last killing frost in the spring and the first killing frost in the fall (U.S. Army Corps of Engineers 1987). A killing frost is a temperature of 28°F or colder. The PRMS model in this study incorporates using the period between the last killing frost in the spring and the first killing frost in the fall as the method for determining the GSL for each year.

Table 2. GCM outputs used in this study from the World Climate Research Programme's CMIP3 multimodel dataset archive. GCM definitions not expanded in the text: Bjerknes Centre for Climate Research Bergen Climate Model (BCC-BCM2.0), Commonwealth Scientific and Industrial Research Organisation Mark version 3.0 (CSIRO Mk3.0), Institute of Numerical Mathematics Coupled Model version 3.0 (INM-CM3.0), and Model for Interdisciplinary Research on Climate 3.2 (MIROC3.2).

GCM*	Description
BCCR-BCM2.0	Bjerknes Centre for Climate Research, Norway
CSIRO Mk3.0	Australia Commonwealth Scientific and Industrial Research Organisation, Australia
CSIRO Mk3.5	Australia Commonwealth Scientific and Industrial Research Organisation, Australia
INM-CM3.0	Institute for Numerical Mathematics, Russia
MIROC3.2(medres)	National Institute for Environmental Studies, Japan

* CMIP3 GCM documentation, references, and links can be found online (http://www-pcmdi.llnl.gov/ipcc/model_documentation/ipcc_model_documentation.php).

3. Modeling methods

The U.S. Geological Survey modeled the hydrologic conditions from 2001 to 2099 in 14 basins across the United States using the PRMS model (Figure 1). These 14 basins have a current or past PRMS model application developed for a variety of reasons (Table 1). Results from global climate models (GCMs) were used in the PRMS model as input data for future conditions. However, the GCM spatial resolution is too coarse for hydrologic modeling at the same scale as the basin models, so GCM precipitation and temperature output were downscaled from a coarse resolution to a finer resolution required by the PRMS models.

A brief description of the development of future conditions and model processing is given here, and a detailed description of the methods is provided elsewhere (Hay et al. 2011). Because of the uncertainty in climate modeling, it is desirable to use more than one GCM in order to obtain a range of potential future climatic conditions. Monthly precipitation and temperature output data from five GCMs were processed and used to calculate the climate fields for the PRMS model (Table 2). For each GCM, one current baseline scenario and three future emission scenarios were used (Table 3). The three future emission scenarios (Table 3) lead to very different patterns in greenhouse gas emissions and concentrations (Alley et al. 2007). The GCM output was obtained from the World Climate Research Programme's Coupled Model Intercomparison Project phase 3 (CMIP3) multimodel dataset archive (Alley et al. 2007).

Climate variables used in the PRMS model were derived by calculating the change in climate from baseline to future conditions simulated by each GCM. The 20C3M baseline scenario for water years 1988–99 (a water year is defined as 1 October of a given year to 30 September of the following year, designated by the year in which it ends) was used to represent baseline climatic conditions (Alley et al. 2007). This 12-yr period of record was selected based on the overlap of the available historic records from the 14 basins included in the national study (Hay et al. 2010). Mean monthly climate variables (percentage change in precipitation and degree changes in air temperature) were computed for 12-yr moving window periods (2001–99) using the 20C3M (1988–99) and the A2, B1, and A1B scenarios (Table 3). A 12-yr moving window, starting in 2001 and ending in 2099, results in 1320 future scenarios [(eighty-eight 12-yr climatologies: one per year starting with

Table 3. General Circulation Model baseline and future emission scenarios chosen for this study (from Alley et al. 2007).

Emission scenario	Description/assumptions
20C3M	Twentieth century climate used to determine baseline (1989–99) conditions
A1B	Very rapid economic growth, a global population that peaks in mid-twenty-first century ,and rapid introduction of new and more efficient technologies with a balanced emphasis on all energy sources
B1	Convergent world, with the same global population as emission scenario A1B, but with more rapid changes in economic structures toward a service and information economy that is more ecologically friendly
A2	Very heterogeneous world with high population growth, slow economic development, and slow technological change

2001–12 and ending with 2088–99) × (3 GCM scenarios) × (5 GCMs)]. A schematic of this process is detailed in Figure 2. Climate variables for PRMS were generated by modifying the daily PRMS precipitation and air temperature inputs (1988–99) with the mean monthly climate variables derived from the GCMs, resulting in 1320 future scenarios for each study area. The first year of each 12-yr simulation was used as PRMS initialization and was not included in the results analysis.

The PRMS model was modified to simulate climate change impacts on GSL. The PRMS model runs in a preprocessing mode to determine the day of the last spring frost and the day of the first fall frost for each year, by hydrologic response unit (HRU) for the period of record of the climate data. The seasonal start and end frost dates are averaged together to create spring and fall frost parameters by HRU in PRMS. The preprocess mode in PRMS calculates basin average spring and fall frost parameters in addition to the HRU parameters. The GSL parameters are appended to the main PRMS parameter file. Standard PRMS simulations use the spring and fall frost parameters to determine when to compute transpiration. During periods of active transpiration, both transpiration and evaporation are calculated in PRMS. If transpiration is inactive, then PRMS only calculates evaporation.

4. Discussion and conclusions

The change in annual GSL (number of days) for each emission scenario and basin is shown in Table 4. All of the basins under all three emission scenarios exhibited an increase in GSL. The largest increases in GSL generally occurred in the three mountainous regions: the Cascades, Sierra Nevada, and the Rockies. The mountainous regions GSL varied from 24 to 76 days for all three scenarios. The Midwest and Southeast regions had the lowest increases in GSL overall (14–39 days), whereas the increases in GSL in the Northeast were between the two extremes (20–43 days). The mean increase in GSL for all basins for the three future emission scenarios was from 27 to 47 days. The 14 basins not only showed an increase in total GSL but also showed a change in the onset and end of the growing season (Table 5). The mountainous basins demonstrate the largest shifts in either the onset or the end of the growing season, whereas the Midwest, Northeast, and Southeast basins exhibit a smaller shift in the timing of the growing season. All basins show an earlier onset of spring and delay in the first fall killing frost.

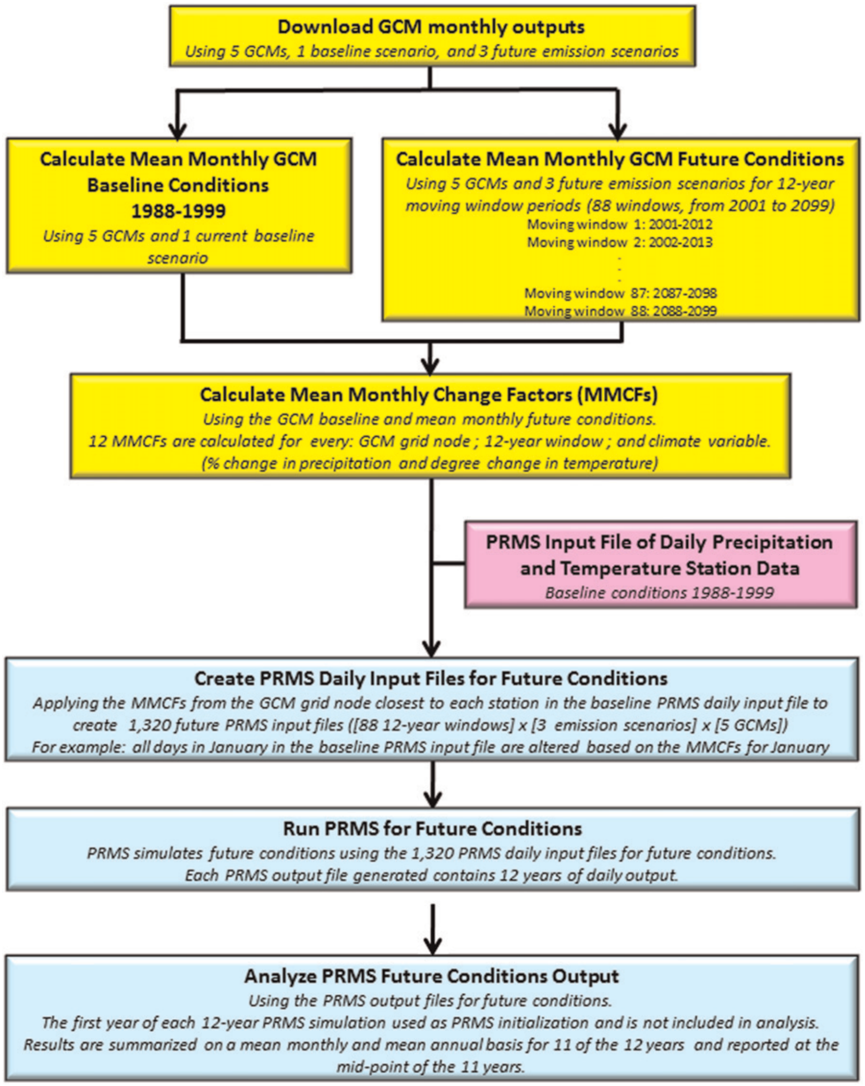

Figure 2. Schematic of the climate change factor method as applied in this study.

Figure 3 shows the change in mean GSL of all basins for each emission scenario through time. The solid colored lines represent the mean value for each of the emission scenarios with the associated color cross-hatch representing the uncertainty associated with the prediction. In general, the results show the model predictions for these selected basins vary largely because of uncertainties in the climate predictions, with the uncertainty increasing as the simulations approach the end of the century (Figure 3).

The projected effects of an increasing GSL on the 14 selected basins are substantial. Table 6 shows the projected change in a number of hydrologically important characteristics by year (slope) and adjusted R^2 (adjR2) based on the central tendencies of the five GCMs for each of the three emission scenarios. The subtables

Table 4. Modeled growing season length increase in days from 2001 to 2099. Values represent average of five GCMs for the three emission scenarios by basin.

		Increase in GSL		
Region	Basin	A2 Days	A1B Days	B1 Days
Cascade	Naches	45	36	24
	Sprague	65	54	43
Sierra Nevada	Sagehen	76	67	51
	Feather	75	63	40
Rockies	Flathead	47	38	28
	East	53	45	30
	Yampa	46	39	25
Midwest	Starkweather	27	20	14
	Black Earth	34	27	18
	Clear	34	27	15
	Trout	39	32	21
Northeast	Cathance	37	29	20
	Pomperaug	43	35	26
Southeast	Flint	33	28	16
Mean value for all basins		47	39	27

show, by variable, changes in slope of the central tendency; the table values set in bold indicate a significant positive trend ($p < 0.05$) and the values set in italics indicates a significant negative trend ($p < 0.05$) for all 14 basins. The adjusted R^2 value gives an indication of the variability around the trend line, with higher adjusted R^2 values having smaller variability. Table 6a shows the GSL statistically has a significant positive trend and low variability. The increasing warming and drying could lead to potential increases in GSL; Table 6b shows that there is a significant positive trend in precipitation in the A1B emission scenario but little positive to

Table 5. Projected change in the beginning and ending of the growing season from 2001 to 2099.

		Spring (days earlier)			Fall (days later)		
Region	Basin	A2 Total days	A1B Total days	B1 Total days	A2 Total days	A1B Total days	B1 Total days
Cascade	Naches	21	18	12	24	18	12
	Sprague	27	24	18	38	30	25
Sierra Nevada	Sagehen	24	20	13	52	47	38
	Feather	19	15	8	56	48	32
Rockies	Flathead	22	19	13	25	19	15
	East	18	15	9	35	30	21
	Yampa	22	19	13	24	20	12
Midwest	Starkweather	15	12	8	12	8	6
	Black Earth	15	12	8	19	15	10
	Clear	16	13	7	18	14	8
	Trout	20	17	10	19	15	11
Northeast	Cathance	18	14	10	19	15	10
	Pomperaug	20	17	12	23	18	14
Southeast	Flint	16	13	7	17	15	9
Mean value for all basins		20	16	11	27	22	16

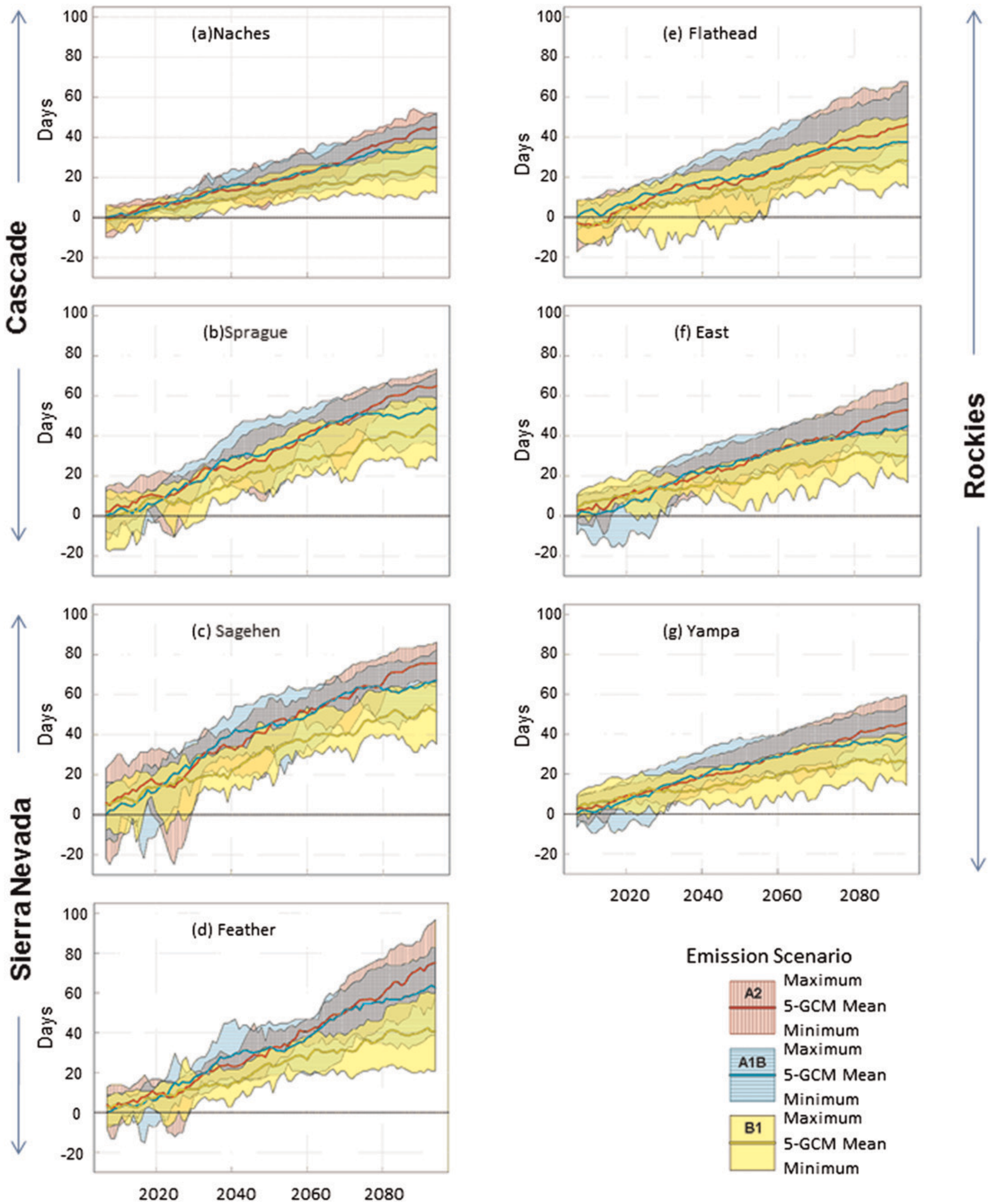

Figure 3. Range in 11-yr moving mean daily growing season values by emission scenario for the 14 basins.

negative trends in both the A2 and B1 emission scenarios with higher variability for all three emission scenarios. The majority of basins under all three emission scenarios exhibited higher minimum and maximum temperatures and evapotranspiration, with decreases in soil moisture and decreased streamflow (Tables 6c–g). These factors and an increasing GSL could lead to variations in water availability,

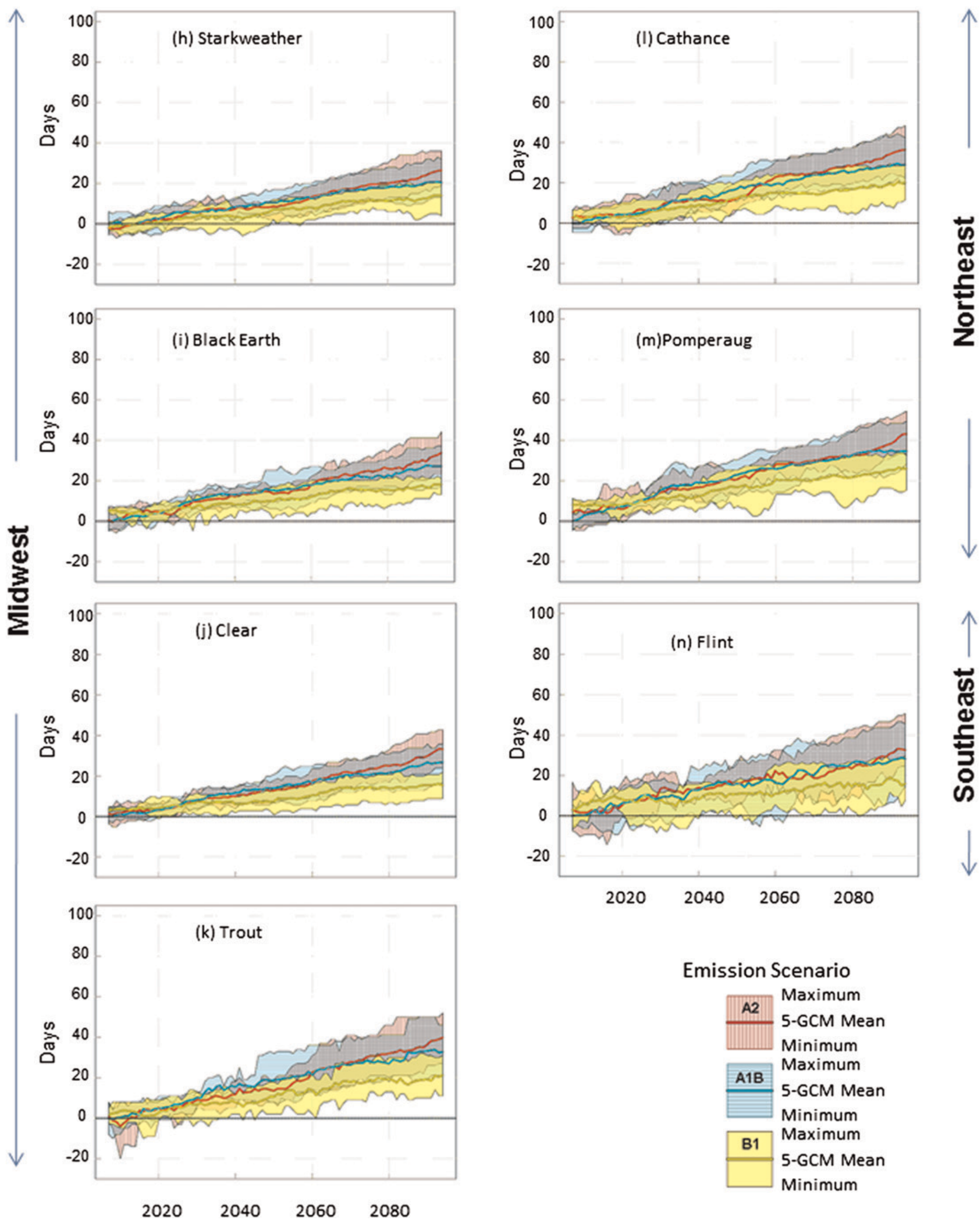

Figure 3. (*Continued*)

which would have a direct impact on agricultural production and water supply in the study basins. An increase in temperature has the potential to impact agricultural production due to the northern migration of competing plants and an increase in insects that is expected to accompany the forecast climate changes (Janetos et al. 2008). In the fire-prone areas of the Rockies and Sierra Nevada study basins, an

Table 6. Projected change by year (slope) and adjR2 based on the central tendencies of the five GCMs for the three emission scenarios by basin: (a) growing season, (b) precipitation, (c) minimum temperature, (d) maximum temperature, (e) evapotranspiration, (f) soil moisture, and (g) streamflow. Italics indicate a significant negative trend, and bold indicates a significant positive trend ($p < 0.05$).

(a) Growing season (days): Length of growing season

		Emission scenario A1B		Emission scenario A2		Emission scenario B1	
Region	Basin	Slope	adjR2	Slope	adjR2	Slope	adjR2
Cascade	Naches	**0.4343**	**0.99**	**0.5173**	**0.98**	**0.2974**	**0.99**
	Sprague	**0.6852**	**0.96**	**0.7669**	**0.99**	**0.54**	**0.98**
Sierra Nevada	Sagehen	**0.7947**	**0.95**	**0.8562**	**0.99**	**0.5801**	**0.98**
	Feather	**0.6285**	**0.98**	**0.7145**	**0.99**	**0.4385**	**0.99**
Rockies	Flathead	**0.4506**	**0.98**	**0.5746**	**0.98**	**0.372**	**0.97**
	East	**0.5515**	**0.97**	**0.5849**	**0.99**	**0.3173**	**0.97**
	Yampa	**0.4625**	**0.97**	**0.5116**	**1**	**0.2786**	**0.97**
Midwest	Starkweather	**0.2533**	**0.99**	**0.3093**	**0.98**	**0.178**	**0.97**
	Black Earth	**0.3057**	**0.97**	**0.3536**	**0.98**	**0.1747**	**0.96**
	Clear	**0.3095**	**0.99**	**0.3546**	**0.98**	**0.1597**	**0.95**
	Trout Lake	**0.3995**	**0.98**	**0.4699**	**0.98**	**0.2378**	**0.94**
Northeast	Cathance	**0.3569**	**0.99**	**0.4008**	**0.97**	**0.2148**	**0.97**
	Pomperaug	**0.4049**	**0.97**	**0.4248**	**0.99**	**0.23**	**0.98**
Southeast	Flint	**0.3221**	**0.97**	**0.3207**	**0.95**	**0.1359**	**0.85**

(b) Precipitation (mm): Area-weighted adjusted precipitation for basin

		Emission scenario A1B		Emission scenario A2		Emission scenario B1	
Region	Basin	Slope	adjR2	Slope	adjR2	Slope	adjR2
Cascade	Naches	**0.0018**	**0.49**	**0.0029**	**0.77**	0.0002	0
	Sprague	**0.0009**	**0.51**	0.0015	0.43	0.0005	0.1
Sierra Nevada	Sagehen	**0.0031**	**0.6**	0.0033	0.16	0.0009	0.03
	Feather	0.0021	0.38	0.0018	0.04	0.0003	0
Rockies	Flathead	**0.004**	**0.87**	**0.0049**	**0.69**	0.0022	0.51
	East	**0.0013**	**0.5**	−0.0007	0.11	0.0011	0.31
	Yampa	**0.0011**	**0.56**	−0.0001	0	0.0004	0.1
Midwest	Starkweather	−0.0006	0.11	0.0004	0.08	0	0
	Black Earth	0.0009	0.21	−0.0007	0.06	−0.0003	0
	Clear	0.0008	0.14	−0.0018	0.25	0.0006	0.02
	Trout Lake	0.0004	0.02	0.0008	0.2	0.0007	0.05
Northeast	Cathance	**0.0019**	**0.56**	**0.0019**	**0.58**	0.0016	0.4
	Pomperaug	0.0019	0.38	0.0002	0	**0.0024**	**0.57**
Southeast	Flint	*−0.0014*	*0.35*	*−0.0047*	*0.72*	0.0008	0.04

(c) Minimum temperature (°C): Basin area-weighted daily minimum temperature

		Emission scenario A1B		Emission scenario A2		Emission scenario B1	
Region	Basin	Slope	adjR2	Slope	adjR2	Slope	adjR2
Cascade	Naches	**0.029**	**0.98**	**0.034**	**0.98**	**0.021**	**0.99**
	Sprague	**0.03**	**0.99**	**0.036**	**0.98**	**0.022**	**0.99**
Sierra Nevada	Sagehen	**0.031**	**0.99**	**0.037**	**0.98**	**0.023**	**0.99**
	Feather	**0.03**	**0.99**	**0.036**	**0.98**	**0.022**	**0.99**
Rockies	Flathead	**0.033**	**0.99**	**0.04**	**0.98**	**0.024**	**0.98**
	East	**0.031**	**0.98**	**0.04**	**0.98**	**0.022**	**0.98**
	Yampa	**0.033**	**0.99**	**0.042**	**0.99**	**0.022**	**0.98**

Table 6. (*Continued*)

(c) Minimum temperature (°C): Basin area-weighted daily minimum temperature

		Emission scenario A1B		Emission scenario A2		Emission scenario B1	
Region	Basin	Slope	adjR2	Slope	adjR2	Slope	adjR2
Midwest	Starkweather	**0.042**	**0.99**	**0.049**	**0.98**	**0.028**	**0.97**
	Black Earth	**0.04**	**1**	**0.048**	**0.99**	**0.024**	**0.97**
	Clear	**0.039**	**0.99**	**0.046**	**0.99**	**0.022**	**0.96**
	Trout Lake	**0.041**	**1**	**0.048**	**0.99**	**0.026**	**0.97**
Northeast	Cathance	**0.035**	**0.99**	**0.041**	**0.98**	**0.02**	**0.98**
	Pomperaug	**0.034**	**1**	**0.04**	**0.99**	**0.019**	**0.99**
Southeast	Flint	**0.03**	**1**	**0.034**	**0.98**	**0.017**	**0.99**

(d) Maximum temperature (°C): Basin area-weighted daily maximum temperature

		Emission scenario A1B		Emission scenario A2		Emission scenario B1	
Region	Basin	Slope	adjR2	Slope	adjR2	Slope	adjR2
Cascade	Naches	**0.028**	**0.97**	**0.033**	**0.97**	**0.023**	**0.99**
	Sprague	**0.03**	**0.97**	**0.037**	**0.98**	**0.024**	**0.99**
Sierra Nevada	Sagehen	**0.031**	**0.98**	**0.04**	**0.98**	**0.024**	**0.98**
	Feather	**0.03**	**0.98**	**0.038**	**0.99**	**0.023**	**0.98**
Rockies	Flathead	**0.031**	**0.98**	**0.04**	**0.99**	**0.024**	**0.98**
	East	**0.037**	**0.99**	**0.049**	**0.99**	**0.022**	**0.95**
	Yampa	**0.035**	**0.99**	**0.047**	**0.99**	**0.023**	**0.97**
Midwest	Starkweather	**0.04**	**0.99**	**0.046**	**0.98**	**0.026**	**0.96**
	Black Earth	**0.04**	**1**	**0.049**	**0.99**	**0.024**	**0.97**
	Clear	**0.041**	**0.99**	**0.051**	**0.99**	**0.023**	**0.96**
	Trout Lake	**0.039**	**0.99**	**0.047**	**0.99**	**0.023**	**0.97**
Northeast	Cathance	**0.033**	**0.99**	**0.038**	**0.98**	**0.018**	**0.98**
	Pomperaug	**0.032**	**1**	**0.039**	**0.99**	**0.017**	**0.99**
Southeast	Flint	**0.034**	**0.99**	**0.043**	**0.98**	**0.018**	**0.95**

(e) Actual evapotranspiration (mm): Evapotranspiration on basin

		Emission scenario A1B		Emission scenario A2		Emission scenario B1	
Region	Basin	Slope	adjR2	Slope	adjR2	Slope	adjR2
Cascade	Naches	0.0005	0.38	**0.001**	**0.77**	**0.0006**	**0.61**
	Sprague	**0.0007**	**0.58**	0.0011	0.65	0.0007	0.49
Sierra Nevada	Sagehen	**0.002**	**0.94**	**0.0021**	**0.84**	**0.0013**	**0.82**
	Feather	**0.0012**	**0.91**	**0.0013**	**0.76**	**0.001**	**0.69**
Rockies	Flathead	**0.0028**	**0.97**	**0.0035**	**0.94**	**0.0023**	**0.94**
	East	**0.0031**	**0.98**	**0.0034**	**0.91**	**0.0025**	**0.92**
	Yampa	**0.0024**	**0.97**	**0.0026**	**0.91**	**0.0017**	**0.96**
Midwest	Starkweather	**0.0012**	**0.75**	**0.0018**	**0.88**	**0.001**	**0.66**
	Black Earth	**0.0027**	**0.92**	**0.0029**	**0.93**	0.0018	0.69
	Clear	**0.0044**	**0.97**	**0.0042**	**0.94**	**0.0029**	**0.89**
	Trout Lake	**0.0018**	**0.93**	**0.0021**	**0.95**	**0.0013**	**0.82**
Northeast	Cathance	**0.0049**	**0.99**	**0.0058**	**0.98**	**0.0029**	**0.98**
	Pomperaug	**0.0045**	**0.99**	**0.0053**	**0.99**	**0.0029**	**0.99**
Southeast	Flint	**0.0013**	**0.75**	**0.0008**	**0.54**	**0.0012**	**0.7**

Table 6. ***(Continued)***

(f) Soil moisture (mm)

Region	Basin	Emission scenario A1B Slope	Emission scenario A1B adjR2	Emission scenario A2 Slope	Emission scenario A2 adjR2	Emission scenario B1 Slope	Emission scenario B1 adjR2
Cascade	Naches	*−0.0344*	*0.69*	*−0.0325*	*0.81*	*−0.0343*	*0.86*
	Sprague	*−0.0315*	*0.56*	−0.0333	0.48	−0.0289	0.37
Sierra Nevada	Sagehen	*−0.1596*	*0.68*	−0.234	0.51	−0.1792	0.53
	Feather	*−0.071*	*0.89*	*−0.0908*	*0.83*	*−0.0564*	*0.69*
Rockies	Flathead	*−0.0456*	*0.69*	*−0.076*	*0.86*	−0.0322	0.38
	East	*−0.0725*	*0.72*	*−0.1258*	*0.82*	−0.0113	0.03
	Yampa	*−0.0852*	*0.84*	*−0.1596*	*0.9*	*−0.0476*	*0.63*
Midwest	Starkweather	*−0.326*	*0.82*	*−0.34*	*0.93*	−0.2087	0.63
	Black Earth	*−0.0549*	*0.93*	*−0.0785*	*0.95*	*−0.0326*	*0.66*
	Clear	*−0.3386*	*0.93*	*−0.5071*	*0.95*	−0.1537	0.55
	Trout Lake	*−0.0217*	*0.95*	*−0.0227*	*0.97*	*−0.0106*	*0.67*
Northeast	Cathance	*−0.0405*	*0.98*	*−0.0456*	*0.93*	*−0.0204*	*0.96*
	Pomperaug	*−0.165*	*0.95*	*−0.2205*	*0.93*	*−0.0534*	*0.64*
Southeast	Flint	*−0.2076*	*0.95*	*−0.2995*	*0.97*	−0.0902	0.56

(g) Streamflow ($m^3\ s^{-1}$): Streamflow from basin

Region	Basin	Emission scenario A1B Slope	Emission scenario A1B adjR2	Emission scenario A2 Slope	Emission scenario A2 adjR2	Emission scenario B1 Slope	Emission scenario B1 adjR2
Cascade	Naches	**0.0561**	**0.59**	**0.0789**	**0.79**	−0.0023	0
	Sprague	0.0107	0.15	0.0225	0.15	−0.0128	0.1
Sierra Nevada	Sagehen	0.0004	0.23	0.0005	0.04	−0.0001	0
	Feather	0.1132	0.16	0.082	0	−0.0378	0
Rockies	Flathead	**0.0547**	**0.41**	0.0676	0.22	−0.001	0
	East	*−0.015*	*0.7*	*−0.0347*	*0.91*	*−0.0118*	*0.51*
	Yampa	*−0.0205*	*0.77*	*−0.0415*	*0.89*	*−0.0211*	*0.67*
Midwest	Starkweather	*−0.0056*	*0.66*	*−0.0047*	*0.75*	−0.0031	0.37
	Black Earth	*−0.0014*	*0.59*	*−0.0028*	*0.75*	−0.0016	0.49
	Clear	*−0.0101*	*0.73*	*−0.0169*	*0.86*	−0.0065	0.48
	Trout Lake	*−0.0015*	*0.61*	*−0.0014*	*0.74*	−0.0004	0.04
Northeast	Cathance	*−0.0029*	*0.78*	*−0.0038*	*0.84*	−0.0012	0.35
	Pomperaug	−0.0061	0.59	*−0.0116*	*0.82*	−0.0012	0.05
Southeast	Flint	*−0.2162*	*0.76*	*−0.4359*	*0.83*	−0.0373	0.02

increase in GSL can cause an increase in tree mortality, which can increase the fuel sources for potential wildfires (Ryan et al. 2008; Fagre et al. 2009). The increase in GSL could increase the amount of water needed for plant growth; Table 6b shows that the model results do not indicate large increases in precipitation for the 14 basins coupled with the predicted small increases in precipitation; and the probability of drought conditions over a longer GSL is increased.

The PRMS model was modified to examine the effects of emission scenarios on the total GSL, as well as the effects on the beginning and end of the GSL periods. Another factor evaluated was the impact of the modified GSL computations on hydrologic flows simulated by the PRMS model. The Clear Creek basin PRMS model was selected to examine the modified GSL results and compare to a GSL fixed baseline condition. Table 7 shows which variables changed when the emission scenario determined by GSL was included in the PRMS simulation. The results show

Table 7. Projected change by year (slope) and adjR^2 based on the central tendencies of the five GCMs for the three emission scenarios for the Clear Creek basin, showing the difference between GSL fixed to baseline conditions and GSL determined by emission scenario.

	Clear Creek basin GSL fixed to baseline conditions						Clear Creek basin GSL determined by emission scenario					
	Scenario SRESa1b		Scenario SRESa2		Scenario SRESb1		Scenario SRESa1b		Scenario SRESa2		Scenario SRESb1	
Variable	Slope	adjR2	Slope	adjR2	Slope	adjR2	Slope	adjR2	Slope	adjR2	Slope	adjR2
Actual evapotranspiration (mm)	0.0038	0.97	0.0036	0.93	0.0026	0.86	0.0044	0.97	0.0042	0.94	0.0029	0.89
Streamflow (m^3 s^{-1})	−0.0083	0.66	−0.0152	0.82	−0.0055	0.4	−0.0101	0.73	−0.0169	0.86	−0.0065	0.48
Soil moisture (mm)	−0.2812	0.92	−0.4400	0.94	−0.1244	0.46	−0.3386	0.93	−0.5071	0.95	−0.1537	0.55
Surface flow (m^3 s^{-1})	−0.00166	0.53	−0.00348	0.74	−0.00102	0.19	−0.0021	0.64	−0.004	0.79	−0.0013	0.26
Subsurface flow (m^3 s^{-1})	−0.00376	0.64	−0.00678	0.81	−0.00271	0.46	−0.0045	0.71	−0.0075	0.84	−0.0031	0.53
Groundwater flow (m^3 s^{-1})	−0.0029	0.75	−0.0049	0.89	−0.0018	0.48	−0.0035	0.80	−0.0055	0.91	−0.0022	0.57
Infiltration (mm)	0.0013	0.44	−0.0007	0.07	0.0009	0.11	0.0015	0.48	−0.0006	0.04	0.001	0.13
Subsurface reservoir inflow (mm)	−0.0013	0.64	−0.0024	0.81	−0.0010	0.46	−0.0016	0.71	−0.0027	0.85	−0.0011	0.53
Groundwater reservoir recharge (mm)	−0.0011	0.73	−0.0019	0.89	−0.0007	0.48	−0.0013	0.79	−0.0021	0.91	−0.0008	0.58
Subsurface reservoir storage (mm)	−0.0098	0.67	−0.0183	0.85	−0.0065	0.44	−0.012	0.74	−0.0204	0.88	−0.0077	0.53
Groundwater reservoir storage (mm)	−0.4023	0.75	−0.6910	0.89	−0.2532	0.48	−0.4921	0.8	−0.7756	0.91	−0.3054	0.57

there is a change in evapotranspiration and in a majority of the flow variables. Slopes increase in the same positive or negative directions when GSL determined by emission scenario is included in the PRMS simulation. In addition, the adjusted R^2, which indicates a smaller variability and increased accuracy of the model, also increases with the inclusion of the emission scenario determined GSL. These results show that the GSL in the PRMS model has an effect on the results of the hydrologic cycle of the Clear Creek basin.

The future growing season length at 14 basins across 11 states were modeled using five general circulation models with three emission scenarios as inputs to the PRMS. The GSL increased in all three climate change emission scenarios though the twenty-first century. The 14 selected basins in the United States have shown an overall increase in GSL ranging from 14 to 76 days by 2099, depending on the emission scenario. The modeled GSLs are positively correlated with forecasted increases in temperature. All climate change emission scenarios evaluated with PRMS showed an increase in temperature through the twenty-first century. The uncertainties and ranges in the increasing temperatures are reflected in the uncertainty and range in the GSL results.

GSL values for Clear Creek basin, 1 of the 14 basins in this study, were calculated for each emission scenario and compared with a (fixed) baseline GSL. As Table 7 shows, there are increasing changes in both flow and evapotranspiration when GSL is compared with the baseline condition.

Changing land cover could impact the GSL of the 14 basins, potentially influencing both temperature and resultant flows. It should be understood that neither the PRMS model nor the GCMs currently account for land-cover change.

The results in this paper represent a method for calculating GSL as a function of climate change emission scenarios. The results show there is a future need to improve PRMS/GCM modeling by including a changing land use/land cover, because this important factor for determining GSL is not represented in this study. This study has shown that GSL does have hydrologic impacts that should be examined in more detail. The increases in GSL that will accompany forecasted increases in temperature are important because they are integrally linked with a range of factors such as phenological events, agricultural production and practices, and water resources across the United States.

References

Alley, R. B., and Coauthors, 2007: Summary for policymakers. *Climate Change 2007: The Physical Science Basis,* S. Solomon et al., Eds., Cambridge University Press, 18 pp.

Backlund, P., D. Schimel, A. Janetos, J. Hatfield, M. G. Ryan, S. R. Archer, and D. Lettenmaier, 2008: Introduction. The effects of climate change on agriculture, land resources, water resources, and biodiversity in the United States, United States Climate Change Science Program Synthesis and Assessment Product 4.3, 11–20.

Barnett, T. P., J. C. Adam, and D. P. Lettenmaier, 2005: Potential impacts of a warming climate on water availability in snow-dominated regions. *Nature,* **438,** 303–309.

Baron, W. R., G. A. Gordon, H. W. Borns Jr., and D. C. Smith, 1984: Frost-free record reconstruction for eastern Massachusetts, 1773-1980. *J. Climate Appl. Meteor.,* **23,** 317–319.

Bjerklie, D. M., J. J. Starn, and C. Tamayo, 2010: Estimation of the effects of land-use and groundwater withdrawals on groundwater recharge and streamflow using the Precipitation

Runoff Modeling System (PRMS) watershed model and the Modular Groundwater Flow Model (MODFLOW) for the Pomperaug River, Connecticut. U. S. Geological Survey Scientific Investigations Rep. 2010-5114, 77 pp.

Brinkman, W. A. R., 1979: Growing season length as an indicator of climatic variations. *Climatic Change,* **2,** 127–138.

Carroll, A. L., S. W. Taylor, J. Régnière, and L. Safranyik, 2003: Effects of climate change on range expansion by the mountain pine beetle in British Columbia, *Proc. Mountain Pine Beetle Symposium: Challenges and Solutions,* Kelowna, Canada, Natural Resources Canada, 223–232.

Caspersen, J. P., S. W. Pacala, J. C. Jenkins, G. C. Hurtt, P. R. Moorcroft, and R. R. Birdsey, 2000: Contributions of land use history to carbon accumulation in U.S. forests. *Science,* **290,** 1148–1151.

Cooter, E. J., and S. K. LeDuc, 1995: Recent frost date trends in the north-eastern USA. *Int. J. Climatol.,* **15,** 65–75.

Dudley, R. W., 2008: Simulation of the quantity, variability, and timing of streamflow in the Dennys River basin, Maine, by use of a Precipitation-Runoff Watershed Model. U.S. Geological Survey Scientific Investigations Rep. 2008-5100, 44 pp.

Fagre, D. B., and Coauthors, 2009: Case studies. Thresholds of climate change in ecosystems, United States Climate Change Science Program Synthesis and Assessment Product 4.2, 15–34.

Haggerty, B. P., and S. J. Mazer, 2008: The Phenology Handbook. University of California, Santa Barbara Phenology Stewardship Program Rep., 43 pp.

Hay, L. E., M. P. Clark, M. Pagowski, G. H. Leavesley, and W. J. Gutowski Jr., 2006a: One-way coupling of an atmospheric and a hydrologic model in Colorado. *J. Hydrometeor.,* **7,** 569–589.

——, G. H. Leavesley, and M. P. Clark, 2006b: Use of remotely-sensed snow covered area in watershed model calibration for the Sprague River, Oregon. *Proc. Joint Eighth Federal Interagency Sedimentation Conf. and Third Federal Interagency Hydrologic Modeling Conf.,* Reno, NV, Subcommittee on Hydrology. [Available online at http://acwi.gov/hydrology/mtsconfwkshops/conf_proceedings/3rdFIHMC/7D_Hay.pdf.]

——, ——, ——, S. L. Markstrom, R. J. Viger, and M. Umemoto, 2006c: Step wise, multiple objective calibration of a hydrologic model for a snowmelt-dominated basin. *J. Amer. Water Resour Assoc.,* **42,** 877–890.

——, G. J. McCabe, M. P. Clark, and J. C. Risley, 2009: Reducing streamflow forecast uncertainty: Application and qualitative assessment of the upper Klamath River basin, Oregon. *J. Amer. Water Resour. Assoc.,* **45,** 580–596.

——, S. L. Markstrom, and C. Ward-Garrison, 2011: Watershed-scale response to climate change through the twenty-first century for selected basins across the United States. *Earth Interactions,* **15.** [Available online at http://EarthInteractions.org.]

Houghton, J. T., Y. Ding, D. J. Griggs, M. Noguer, P. J. van der Linden, X. Dai, K. Maskell, and C. A. Johnson, Eds., 2001: *Climate Change 2001: The Scientific Basis*. Cambridge University Press, 881 pp.

Janetos, A., L. Hansen, D. Inouye, B. P. Kelly, L. Meyerson, B. Peterson, and R. Shaw, 2008: Biodiversity. The effects of climate change on agriculture, land resources, water resources, and biodiversity in the United States, United States Climate Change Science Program Synthesis and Assessment Product 4.3, 151–182.

Joos, F., I. C. Prentice, and J. I. House, 2002: Growth enhancement due to global atmospheric change as predicted by terrestrial ecosystem models: Consistent with U.S. forest inventory data. *Global Change Biol.,* **8,** 299–303.

Koczot, K. M., A. E. Jeton, B. J. McGurk, and M. D. Dettinger, 2005: Precipitation-runoff processes in the Feather River basin, northeastern California, with prospects for streamflow predictability, water years 1971-97. U.S. Geological Survey Scientific Investigations Rep. 2004-5202, 82 pp.

Kunkel, K. E., D. R. Easterling, K. Hubbard, and K. Redmond, 2004: Temporal variations in frost-free season in the United States: 1895–2000. *Geophys. Res. Lett.,* **31,** L03201, doi:10.1029/2003GL018624.

Logan, J. A., J. Regniere, and J. A. Powell, 2003: Assessing the impacts of global warming on forest pest dynamics. *Front. Ecol. Environ.,* **1,** 130–137.

Markstrom, S. L., R. G. Niswonger, R. S. Regan, D. E. Prudic, and P. M. Barlow, 2008: GSFLOW—Coupled ground-water and surface-water flow model based on the integration of the Precipitation-Runoff Modeling System (PRMS) and the Modular Ground-Water Flow Model (MODFLOW-2005). U.S. Geological Survey Techniques and Methods 6-D1, 240 pp.

Mastin, M. C., and J. J. Vaccaro, 2002: Watershed models for decision support in the Yakima River Basin, Washington. U.S. Geological Survey Open-File Rep. 2002-404, 46 pp.

McCabe, G. J., and L. E. Hay, 1995: Hydrological effects of hypothetical climate change in the East River basin, Colorado. *Hydrol. Sci. J.,* **40,** 1–16.

McKenzie, D., A. E. Hessl, and D. L. Peterson, 2001: Recent growth of conifer species of western North America: Assessing spatial patterns of radial growth trends. *Can. J. For. Res.,* **31,** 526–538.

Parmesan, C., and G. Yohe, 2003: A globally coherent fingerprint of climate change impacts across natural systems. *Nature,* **421,** 37–42.

Ryan, M. G., and Coauthors, 2008: Land resources: Forest and arid lands. The effects of climate change on agriculture, land resources, water resources, and biodiversity in the United States, United States Climate Change Science Program Synthesis and Assessment Product 4.3, 75–120.

U.S. Army Corps of Engineers, 1987: Corps of Engineers wetlands delineation manual. U.S. Army Corps of Engineers Tech. Rep. Y-87-1, 117 pp.

Viger, R. J., L. E. Hay, J. W. Jones, and G. R. Buell, 2010: Accounting for large numbers of small water bodies in the application of the Precipitation-Runoff Modeling System in the Flint River basin, Georgia. U.S. Geological Survey Open File Rep. 2010-5062, 37 pp.

Vining, K. C., 2002. Simulation of streamflow and wetland storage, Starkweather Coulee Subbasin, North Dakota, Water Years 1981-98. U.S. Geological Survey Water-Resources Investigations Rep. 02-4113, 28 pp.

Wang, J. Y., 1963: *Agricultural Meteorology.* Pacemaker Press, 693 pp.